JBIC Journal of Biological Inorganic Chemistry (2020) 25:949–962
https://doi.org/10.1007/s00775-020-01816-w

ORIGINAL PAPER

Development of an improved Amplex Red peroxidation activity assay for screening cytochrome P450 variants and identification of a novel mutant of the thermophilic CYP119

M. Semih Başlar[1] · Tuğçe Sakallı[2] · Gülce Güralp[1] · Ekin Kestevur Doğru[1] · Emre Haklı[2] · Nur Basak Surmeli[1]

Received: 27 April 2020 / Accepted: 30 August 2020 / Published online: 13 September 2020

Abstract

Biocatalysts are increasingly utilized in the synthesis of drugs and agrochemicals as an alternative to chemical catalysis. They are preferred in the synthesis of enantiopure products due to their high regioselectivity and enantioselectivity. Cytochrome P450 (P450) oxygenases are valuable biocatalysts, since they catalyze the oxidation of carbon–hydrogen bonds with high efficiency and selectivity. However, practical use of P450s is limited due to their need for expensive cofactors and electron transport partners. P450s can employ hydrogen peroxide (H_2O_2) as an oxygen and electron donor, but the reaction with H_2O_2 is inefficient. The development of P450s that can use H_2O_2 will expand their applications. Here, an assay that utilizes Amplex Red peroxidation, to rapidly screen H_2O_2-dependent activity of P450 mutants in cell lysate was developed. This assay was employed to identify mutants of CYP119, a thermophilic P450 from *Sulfolobus acidocaldarius*, with increased peroxidation activity. A mutant library of CYP119 containing substitutions in the heme active site was constructed via combinatorial active-site saturation test and screened for improved activity. Screening of 158 colonies led to five mutants with higher activity. Among improved variants, T213R/T214I was characterized. T213R/T214I exhibited fivefold higher k_{cat} for Amplex Red peroxidation and twofold higher k_{cat} for styrene epoxidation. T213R/T214I showed higher stability towards heme degradation by H_2O_2. While the K_m for H_2O_2 and styrene were not altered by the mutation, a fourfold decrease in the affinity for another substrate, lauric acid, was observed. In conclusion, Amplex Red peroxidation screening of CYP119 mutants yielded enzymes with increased peroxide-dependent activity.

Electronic supplementary material The online version of this article (https://doi.org/10.1007/s00775-020-01816-w) contains supplementary material, which is available to authorized users.

✉ Nur Basak Surmeli
nursurmeli@iyte.edu.tr

[1] Department of Bioengineering, İzmir Institute of Technology, Gülbahçe, Urla, Izmir, Turkey

[2] Program in Biotechnology and Bioengineering, İzmir Institute of Technology, Gülbahce, Urla, Izmir, Turkey

Graphic abstract

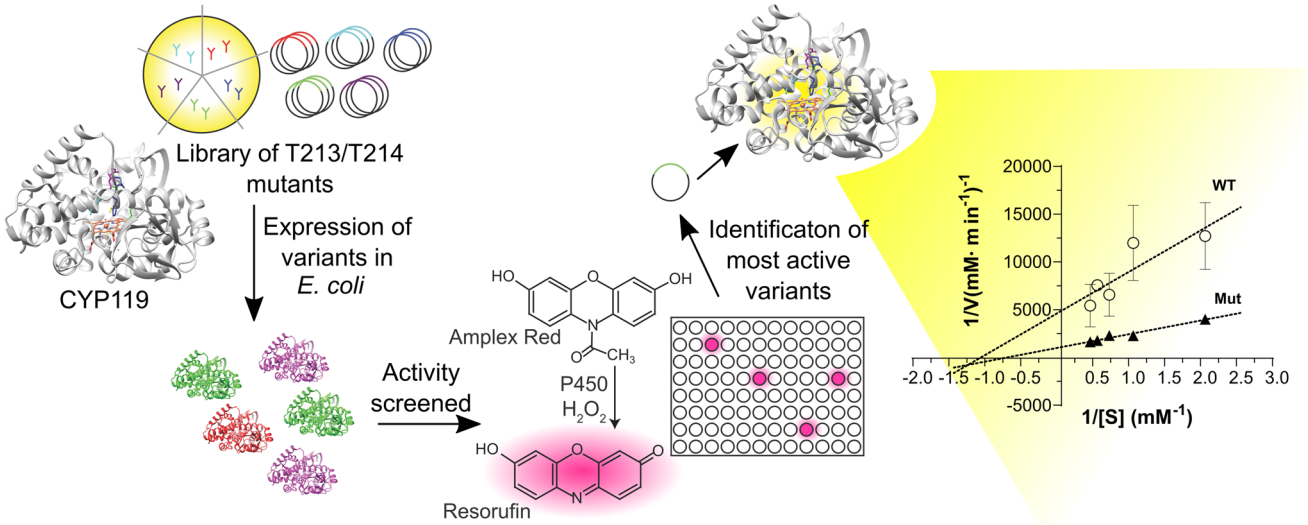

Keywords Cytochrome · Biocatalysis · Protein engineering · Enzyme kinetics · Heme

Abbreviations

P450	Cytochrome P450
HRP	Horseradish peroxidase
WT	Wild type
IPTG	Isopropyl β-D-1-thiogalactopyranoside
NAD(P)H	Nicotinamide adenine dinucleotide phosphate
CAST	Combinatorial active-site saturation test
PMSF	Phenylmethylsulfonyl fluoride
EDTA	Ethylenediaminetetraacetic acid
DMSO	Dimethyl sulfoxide
TBHP	*Tert*-butyl hydroperoxide
FAD	Flavin adenine dinucleotide
FMN	Flavin mononucleotide
RCSB PDB	The Research Collaboratory for Structural Bioinformatics Protein Data Bank
PDB ID	Protein data bank identity
REU	Rosetta energy unit

Introduction

Biocatalysis is the chemical process whereby enzymes catalyze reactions between organic components. Most significant features of enzymes are their high regioselectivity and enantioselectivity. These properties have expanded the utilization of enzymes in the pharmaceutical and agrochemical industry [1]. Developments in biotechnology have led to engineered biocatalysts capable of performing reactions that are challenging with chemical catalysts. Amongst biocatalysts, P450s have attracted attention due to their capability to catalyze the oxidation of "unactivated" hydrocarbons with high efficiency and selectivity. Indeed, P450 enzymes are currently used in the synthesis of steroids and statins [2, 3].

P450s most commonly catalyze the insertion of a single oxygen atom into an organic substrate using molecular oxygen (O_2) and the hydride (H^-) donor nicotinamide adenine dinucleotide phosphate (NAD(P)H). P450s require protein partners to deliver the electrons from the expensive cofactor NAD(P)H. Since the expression and purification of electron transfer proteins' cost resources and energy, whole-cell catalysis is generally employed for the synthesis of pharmaceuticals [4, 5]. This limits the P450 enzymes that can be utilized, since not all host organisms are amenable to industrial processes. P450s can also employ hydrogen peroxide (H_2O_2) as an oxygen donor and electron acceptor [6]. This eliminates the need for expensive cofactors and electron transfer partners. Nevertheless, the reaction with H_2O_2 is inefficient, except for a few P450s such as P450BSβ [7]. General acid/base residues at the heme distal site are crucial for the generation of compound I, which is responsible for H_2O_2-dependent oxidation [6]. The development of P450 enzymes that can utilize H_2O_2 efficiently will lead to an expansion of the application of P450s as biocatalysts.

To date, protein engineering approaches have mostly focused on the bacterial CYP102A1 (P450BM3) and CYP101A1 (P450CAM), because they are highly soluble and active when expressed in *E. coli* [8]. Since it is advantageous to obtain P450 enzymes that can utilize H_2O_2, laboratory evolution of P450CAM to enhance the rate of

H_2O_2-driven naphthalene hydroxylation has been attempted [9]. However, isolation and characterization of this mutant have revealed that it generates only trace amounts of hydroxylated naphthalene [10]. P450BM3 is expressed with the electron transfer FAD/FMN reductase domain and the P450 monooxygenase domain on a single polypeptide, which makes optimization of P450BM3 challenging as mutations can independently affect coupling efficiency and activity.

CYP119 is a P450 from the thermoacidophilic archaeon *Sulfolobus acidocaldarius*. *Sulfolobus* sp. are sulfur utilizing organisms that have optimum growth conditions of between 78 and 86 °C and pH 2–4 [11, 12]. Since the thermophilic enzymes have increased stability toward mutations, high temperature, and extreme pH, they have more potential applications compared to mesophilic enzymes. CYP119 is one of the most extensively studied thermostable P450s and its molecular structure has been determined by X-ray crystallography [13]. The natural substrates and redox partners of CYP119 are currently unknown. However, CYP119 can oxidize lauric acid using the auxiliary redox partner proteins putidaredoxin and putidaredoxin reductase with NADH as an electron donor [14]. CYP119 can also use H_2O_2 as an oxidant via the peroxide shunt pathway with low efficiency. Previous studies have shown that CYP119 can catalyze epoxidation of styrene, hydroxylation of lauric acid, chemical dehalogenation, and electrochemical reduction of nitrite, nitric oxide, and nitrous oxide [15]. Here, CYP119 mutants were screened for peroxidation activity to develop a biocatalyst that can utilize H_2O_2 more efficiently.

Even though natural redox partner and substrate(s) of CYP119 are unknown, previous studies have shown that CYP119 can catalyze the peroxidation of Amplex® Red (*N*-acetyl-3,7-dihydroxyphenoxazine) in the presence of H_2O_2 [15, 17, 18]. Amplex® Red is a non-fluorescent reagent, which is converted by oxidation to a red fluorescent product resorufin that has excitation maximum at 571 nm and emission maximum at 585 nm [19–21]. Amplex® Red has commonly been used as a probe in the detection of H_2O_2 in conjunction with horseradish peroxidase (HRP) [28]. However, due to the complex mechanism of Amplex® Red oxidation and low activity of Amplex® Red with P450s, it has never been used in cell lysates to screen for activity of mutant P450s. We optimized the Amplex® Red screen to assess CYP119 peroxidase activity. Improved catalytic activity of the mutant library was measured by an assay involving the conversion of Amplex® Red to resorufin in the presence of H_2O_2.

A mutant library of CYP119 was generated to screen for increased peroxidation activity using the optimized assay. Since mutations in the active site are expected to have a much larger effect on activity, we decided to have a targeted approach. The combinatorial active-site saturation test (CAST) method was used to generate the mutant library. In this approach pairs of amino acids within a defined proximity—sufficiently close to interact—are randomized pairwise [16]. The effectiveness of the CAST method depends highly on the selection of the right amino acids to be randomized. Previous studies have shown that Thr213 and Thr214 residues play important roles in the active site, but they are not critical for thermal stability [11]. Therefore, these residues were selected for targeted mutation.

Here, we report the generation of a mutant library of CYP119 containing substitutions at the Thr213 and Thr214 positions as well as the development of an effective screening method utilizing Amplex® Red as a substrate to measure improved H_2O_2-dependent catalytic activity of CYP119 variants. Screening of the mutant library resulted in five mutants with improved activity compared to wild-type (WT) CYP119. Among five improved mutants, further characterization of the T213R/T214I was performed. T213R/T214I showed improved activity toward Amplex® Red peroxidation and styrene epoxidation and exhibited improved stability against H_2O_2 degradation.

Materials and methods

Expression of WT CYP119 and T213R/T214I mutant

Expression vector containing WT CYP119 (pET11a + CYP119) was a gift from Teruyuki Nagamune (Addgene plasmid # 66131) [22]. For expression of WT CYP119, pET11a + CYP119 plasmid was transformed into *E. coli* BL21 (DE3) cells. Recombinant *E. coli* BL21 (DE3) was cultured in 10 mL of Lysogeny Broth (LB, 10 g L^{-1} tryptone, 5 g L^{-1} yeast extract, and 10 g L^{-1} NaCl) with 0.1 g L^{-1} ampicillin. The culture was incubated overnight at 37 °C and 220 rpm in a shaking incubator. Overnight culture (5 mL) was inoculated to 500 mL of 2xYT Medium Broth (16 g L^{-1} tryptone, 10 g L^{-1} yeast extract, and 5 g L^{-1} NaCl at pH 6.8) with 0.1 g L^{-1} ampicillin and grown at 37 °C with 220 rpm shaking until optical densities reached ~ 0.7 at OD_{600}. Expression of WT CYP119 was induced with 1 mM isopropyl β-D-1-thiogalactopyranoside (IPTG) for 32 h at 30 °C. The cells were harvested by centrifugation at 3800 rpm for 30 min and pellets were stored at − 80 °C until purification.

Enrichment of WT CYP119

The frozen cell pellets obtained were dissolved in lysis buffer (0.1 M NaCl, 0.2 mM phenylmethylsulfonyl fluoride (PMSF), 1 mM benzamidine HCl, and 50 mM potassium phosphate at pH 7.5). Cells were ultrasonicated, and cell lysate was incubated at 65 °C for 1 h, followed by centrifugation at

12,000 rpm for 20 min at room temperature. WT CYP119 was enriched in the collected supernatant.

Generation of mutant library

Generation of mutant library was accomplished with the polymerase chain reaction (PCR) using Q5 Site-Directed Mutagenesis Kit (BioLabs). Degenerate primers that contain NDT codons at Thr213–Thr214 positions (GGGTAA TGAGNDTNDTACTAACTTAATATCAAACTC TGTTAT TG and GCTATGAGAAGTAAAATAATGTATC) were used. CYP119 mutant library was created by heat-shock transformation of the plasmids containing mutant genes to *E. coli* BL21 (DE3). Colonies were randomly selected from the library; their plasmids were isolated and then sequenced to confirm mutations at desired sites.

Peroxidase activity of WT CYP119 and T213R/T214I mutant with Amplex® Red

Amplex® Red (Thermo Fisher Scientific) peroxidation experiments were carried out as previously described [15, 18]. Briefly, reaction mixtures included 10 µM Amplex® Red, 1.5 mM H_2O_2, 1 mM ethylenediaminetetraacetic acid (EDTA), and 1.5 µM WT CYP119 or variants in 50 mM potassium phosphate at pH 7.4. The reactions occurred at room temperature. Production of resorufin was analyzed by monitoring fluorescence emission (570 nm excitation and 585 nm emission) or absorbance at 570 nm ($\varepsilon_{570nm} = 54\ mM^{-1}\ cm^{-1}$).

Development of screening method

E. coli BL21 (DE3) cells that contain plasmids with WT or mutant CYP119 and empty pET20b genes were grown overnight, in LB media (5 mL) containing 0.1 g L^{-1} ampicillin, at 37 °C with moderate shaking. Each culture (30 µL) was inoculated to 2xYT (8 mL) media containing 0.1 g L^{-1} ampicillin and were grown until reaching $OD_{600} \sim 0.7$ at 37 °C with moderate shaking. A final concentration of 1 mM IPTG was added to each culture media. Protein expression was induced for 32 h at 30 °C with moderate shaking. Aliquots from each culture (3 mL) were harvested by centrifugation and kept at − 80 °C for SoluLyse (protein extraction reagent, Genlantis) treatment or sonication processes.

Harvesting of protein by sonication was done by dissolving cell pellets in lysis buffer (300 µL) and disrupting cells by sonication. Lysed cells were heat-treated at 65 °C for 1 h and then centrifuged to enrich CYP119 in supernatant. Collected supernatants from each culture were used in Amplex® Red peroxidation activity assay. A reaction volume of 100 µL contains 50 µL of extracted enzyme and 50 µL of reaction mixture 1 (1 mM H_2O_2, 50 µM Amplex® Red, and 50 mM potassium phosphate buffer, pH 7.4).

Harvesting of protein by SoluLyse treatment was done by dissolving pellets in SoluLyse reagent (300 µL) and then centrifuged to obtain proteins in the supernatant. Collected supernatants were used in the Amplex® Red peroxidation activity assay. A reaction volume of 100 µL contains 50 µL of extracted enzyme and 50 µL of reaction mixture 1.

For both methods, proteins extracted from *E. coli* BL21 (DE3) cells that contain pET20b were used as a negative control group and HRP was used as a positive control group. Mixtures were inoculated for 30 min at 25 °C; fluorescence emission values of resorufin between 550 and 700 nm were measured with excitation at 530 nm. Each reaction was done quintuplicate; graphs were created using mean values of duplicates.

Rapid screening of CYP119 mutant library

The rapid screening method used for CYP119 mutant library is summarized in Fig. 1. 96-well cell culture plates that contain 140 µL LB media with 0.1 g L^{-1} ampicillin in each well were inoculated with *E. coli* BL21 (DE3) bacteria that have plasmids of WT or mutant CYP119 or pET20b. Plates were incubated overnight at 37 °C with moderate shaking. 3 µL of each culture was transferred to 96 deep well plate in a triplicate manner, each well containing 500 µL of 2xYT media with 0.1 g L^{-1} ampicillin. Cultures were incubated at 37 °C with moderate shaking until reaching $OD_{600} \sim 0.7$ value. A final concentration of 1 mM IPTG was added to each culture in two of the copy plates to induce protein expression and

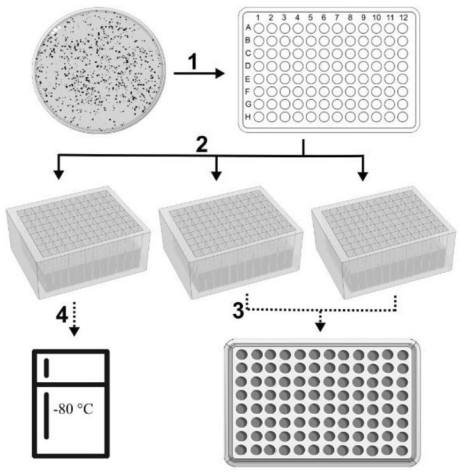

Fig. 1 Steps of the rapid screening method. 1. Transfer of mutant colonies from LB agar plates into 96-well plates that contain LB media in each well. 2. Transfer of grown cultures to 96 deep well plates that contain 2xYT media in each well. 3. Visualization of peroxidation activity of CYP119 variants. 4. Glycerol cell stocks of grown cultures for further use of variants

cultures were incubated at 30 °C for 20 h with moderate shaking. Culture plates were centrifuged at 15,000 rpm for 5 min. Pellets were kept in − 80 °C freezer overnight to help with cell lysing. Pellets were suspended in 50 µL of SoluLyse reagent. Duplicates were merged in a microcentrifuge tube and incubated at 25 °C with moderate shaking for 10 min. Proteins were enriched in the supernatant by centrifugation at 15,000 rpm for 10 min. Collected supernatants were used in Amplex® Red peroxidation activity assay. The third copy plate was kept at − 80 °C after 50% glycerol was added to cultures in a 1:1 volume ratio for traceback.

Amplex® Red peroxidation activity assay in the rapid screening

Amplex® Red peroxidation activity assay has a total of 100 µL reaction volume that consist of 50 µL of enzyme extracted with SoluLyse reagent and 50 µL of reaction mixture 2 (1 mM H_2O_2, 10 µM Amplex® Red, and 50 mM potassium phosphate buffer, pH 7.4). 1:1 v/v SoluLyse reagent and potassium phosphate buffer were used as blank, 1:1 v/v potassium phosphate buffer, and reaction mixture 2, and proteins extracted from *E. coli* BL21 (DE3) cells that contain pET20b mixed with reaction mixture 2 were used as negative controls. The positive control was 1 µU of HRP in 1:1 v/v potassium phosphate buffer and reaction mixture 2. Samples were incubated at 25 °C for 10 min. Fluorescence emission by resorufin was measured at 595 nm with FLUOstar Omega (BMG LABTECH).

Confirmation of improved activity mutant enzymes

Mutant enzymes that exhibited improved activity were picked and grown from the third replicate plate. LB media (5 mL) containing 0.1 g L^{-1} ampicillin were inoculated with improved activity mutant enzymes. Cultures were grown overnight at 37 °C with moderate shaking. 2xYT media (8 mL) containing 0.1 g L^{-1} ampicillin were inoculated with 30 µL of cultures. Upon reaching OD_{600} ~ 0.7, a final concentration of 1 mM IPTG was added to cultures. 3 mL of cultures were incubated for 25 h at 30 °C with moderate shaking. Harvesting was done by centrifugation at 15,000 rpm for 10 min. Pellets were resuspended in 300 µL of SoluLyse reagent and incubated at 25 °C for 10 min with moderate shaking. Proteins were enriched in the supernatant by centrifugation. Collected supernatants were subjected to Amplex® Red peroxidation activity assay.

Isolation and purification of WT CYP119 and T213R/T214I mutant

The frozen cell pellets of WT CYP119 and T213R/T214I mutant were resuspended with lysis buffer (150 mM NaCl, 10 mM imidazole, 0.2 mM PMSF, 1 mM benzamidine HCl, 50 mM potassium phosphate buffer, and pH 7.5). Cells were lysed by sonication and incubated in water bath at 60 °C for 1 h. Lysate was then centrifuged at 3900 rpm for 1.5 h at 4 °C. WT CYP119 was isolated from the supernatant by precipitation with ammonium sulfate (60%) and dissolved with potassium phosphate buffer (50 mM potassium phosphate buffer, 20 mM NaCl, 5% glycerol, and pH 7.5) and dialyzed against the same buffer. T213R/T214I mutant pellets were dissolved with triethanolamine buffer (50 mM) at pH 7.3 and desalted with PD 10 desalting column. 10 µL samples of WT and T213R/T214I were taken for purity analysis by SDS-PAGE (Figure S1). WT CYP119 and the T213R/T214I mutant concentrations were calculated based on the extinction coefficient of CYP119 ($\varepsilon_{415nm} = 104$ mM^{-1} cm^{-1}).

Electronic spectroscopy

All spectra were recorded on a UV-1600PC Scanning Spectrophotometer at room temperature. The UV–Visible spectra of WT CYP119 and T213R/T214I mutant were obtained in 50 mM potassium phosphate buffer at pH 7.4.

Kinetic analysis of Amplex® Red peroxidation by WT CYP119 and T213R/T214I mutant

Amplex® Red peroxidation was performed with WT CYP119 and the T213R/T214I mutant and absorbance change was followed at 570 nm. Reaction mixtures included 10 µM Amplex® Red, 1.5 mM H_2O_2, 1 mM EDTA, and 1.5 µM of enzyme (CYP119 or T213R/T214I mutant) in 50 mM potassium phosphate at pH 7.4. UV–Visible spectra were taken at 0, 2, 5, 10, 20, 30, 45, 60, 90, and 120 min after the addition of H_2O_2. Amplex® Red Reactions with WT CYP119 and T213R/T214I mutant were analyzed under different H_2O_2 concentrations (0.5–2.5 mM) for the determination of kinetic parameters. The initial rate was calculated for each H_2O_2 concentration by linear fitting. A Lineweaver–Burk plot is shown for comparison, and kinetic parameters were obtained by nonlinear fitting of the data to Michaelis–Menten equation.

Substrate binding study

Binding constants of WT CYP119 and T213R/T214I mutant were determined at room temperature by difference spectroscopy. Enzyme solutions for WT CYP119 (1.5 µM) or T213R/T214I (1.5 µM) were prepared in 50 mM potassium phosphate buffer at pH 7.4. Enzyme solutions were kept for 10 min at room temperature and divided into two glass cuvettes. Lauric acid in a dimethyl sulfoxide (DMSO) stock solution was titrated into the sample cuvettes containing WT CYP119 and T213R/T214I mutant. The concentration of DMSO in

the cuvette did not exceed 1% of the initial volume. Equal amounts of DMSO were added to the reference cuvette. The absorbance shift between 386 and 418 nm was followed. The shift was plotted against substrate concentration by nonlinear fitting. K_d value was calculated by plotting the shift against substrate concentration to quadratic equation [23]:

$$\Delta A = A_{\max}\left(\frac{K_d + [E] + [L] - \sqrt{\left(K_d + [E] + [L]\right)^2 - 4[E][L]}}{2[E]}\right)$$

Styrene epoxidation

Styrene epoxidation was performed at room temperature in closed glass vials for 10 min. 100 µl reaction mixture contained 12.5 µM CYP119, variable concentrations of styrene (3–7 mM), and 7 mM tert-butyl hydroperoxide (TBHP) as oxidant in 50 mM phosphate buffer (pH 7.4). The reaction was stopped by adding acetonitrile (900 µL). The reaction mixture was analyzed by high-performance liquid chromatography (HPLC) on a Thermo Scientific Ultimate 3000 coupled with a UV detector fixed at 220 nm. 25 cm Nucleodur C18 column (Macherey–Nagel) was used with 3:7 ddH_2O:acetonitrile as the mobile phase. The retention times of styrene and styrene oxide were determined as 6.5 min and 4.27 min, respectively. Solutions containing known amounts of (±)-styrene oxide were used to generate standard curves for product quantitation.

Reactions of WT CYP119 and T213R/T214I mutant with hydrogen peroxide

Hydrogen peroxide (H_2O_2) reactions were performed with WT CYP119 and T213R/T214I mutant, and absorbance was followed at 414 nm. Reaction mixtures included 1.5 mM H_2O_2, 1 mM EDTA, and 1.5 µM of enzyme (CYP119 or T213R/T214I mutant) in 50 mM potassium phosphate at pH 7.4. UV–Visible spectra were taken at 0, 2, 5, 10, 20, 30, and 45 min after the addition of H_2O_2.

Molecular modeling and docking of Amplex® Red to WT CYP119 and T213R/T214I mutant

The crystal structure of WT CYP119 (PDB ID: 1F4T) was obtained from the RCSB PDB database [13]. The PyRosetta program was used for creating mutations on the structure of WT CYP119 enzyme [24]. Mutations were applied to WT CYP119 structure using the TaskFactory module of PyRosetta. Conformation of mutant residues was optimized with the PackRotamersMover function according to the "REF2015" score function. WT CYP119 and T213R/T214I mutant structures were energy minimized according to FastRelax protocol using "REF2015" as energy function before ligand docking. Ligand docking was performed with the DockMCMProtocol of PyRosetta. 1000 rounds of docking were performed for each structure and docking scores were calculated according to PyRosetta energy function, "ligand". Dock models with the lowest Rosetta Energy Unit (REU) scores were selected to analyze ligand–protein interactions. All images were created with the UCSF Chimera software [25].

Results

Peroxidation of Amplex® Red by CYP119

Previous studies have shown that CYP119 has peroxidase activity with Amplex® Red as a substrate and this activity can be monitored by fluorescence spectroscopy [15, 18]. Oxidation of Amplex® Red by peroxidase results in the formation of the fluorescent compound resorufin, which emits fluorescence at 585 nm when excited at 571 nm.

Peroxidase activity of CYP119 was assayed in cell extracts after cell lysis by sonication and enrichment of CYP119 by heat treatment. WT CYP119 can be obtained approximately 70–80% pure through this method (Figure S2). Enriched CYP119 (2.5 µM) showed oxidation of Amplex® Red (50 µM) using H_2O_2 as an oxidant (1 mM) at room temperature in sodium phosphate buffer (50 mM) at pH 7.4. The fluorescence spectra of the resorufin product obtained are shown in Fig. 2. Based on this result, the oxidation of Amplex® Red by CYP119 was selected for library screening for peroxidation activity.

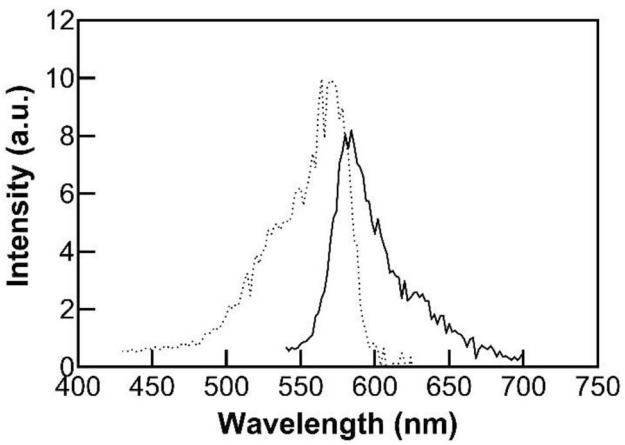

Fig. 2 The fluorescence spectra of the resorufin produced by the reaction of enriched WT CYP119 (2.5 µM), Amplex® Red (50 µM), and H_2O_2 (1 mM) in 50 mM sodium phosphate buffer at pH 7.4. The resorufin spectra are shown for 570 nm excitation (dash) and 585 nm emission (solid), respectively

Screening method for selection of CYP119 mutants for improved peroxidation activity

Obtaining enriched CYP119 by sonication and heat treatment is time-consuming for a rapid activity assay. To develop a feasible screening method, we decided to use SoluLyse treatment as described in the Materials and methods section. The peroxidase activity of enriched CYP119 obtained by sonication as described above was compared with activity observed in the cell lysate obtained with SoluLyse method (Figure S3). In both methods, proteins extracted from *E. coli* BL21 (DE3) containing WT or mutant CYP119 genes were mixed with a reaction mixture (1 mM H_2O_2, 10 µM Amplex® Red, and 1 mM EDTA in 50 mM pH 7.4 potassium phosphate buffer) and incubated at room temperature. Cells that have empty pET20b plasmid were used as a control group. Fluorescence emission of the product resorufin was followed at 585 nm for all samples. As seen in Figure S3, the fluorescence obtained by the SoluLyse method was comparable to enrichment treatment for WT, mutant CYP119, and pET20b control. Therefore, SoluLyse treatment method was used in our assay.

Construction of CYP119 mutant library for screening peroxidase activity

Previous studies have shown that residues Thr213 and Thr214 were important for the peroxidase activity of CYP119 [11]. Therefore, CYP119 mutant library was created by applying the CAST method to the amino acids Thr213 and Thr214 [16]. The nucleotides coding the two threonine residues were mutated to NDT codons coding for 12 amino acids (Phe, Leu, Ile, Val, Tyr, His, Asn, Asp, Cys, Arg, Ser, and Gly). To test if there is any mutational bias in the library, 31 colonies were selected at random and sequenced. The sequences obtained were analyzed by substitution analysis, as seen in Fig. 3, no mutational bias was observed in the mutant library.

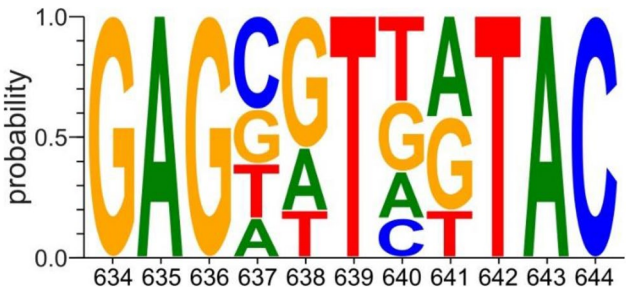

Fig. 3 Substitution analysis of 31 variants of CYP119, at Thr213 (637-639), and Thr214 (640-642) mutation sites [11]. Mutations created using NDT codons. Created using WebLogo3 [26]

Screening of CYP119 mutant library

After the construction of the mutant library, CYP119 mutants were screened for improved peroxidation activity as described in the Materials and method section (Fig. 4). After 10 min of incubation at room temperature, fluorescence emitted by resorufin in each well was measured. Incubation for longer than 10 min did not result in significant changes in fluorescence (results not shown). HRP (1 µUnits) with the reaction mixture 2 (10 µM Amplex® Red and 1 mM H_2O_2 in 50 mM pH 7.4 potassium phosphate buffer) was used as a positive control. Cells harboring empty pET20b plasmid in reaction mixture 2 were used as the negative control.

Peroxidation activity assay with Amplex® Red was performed on 158 mutants to determine variants with improved activity. As shown in Fig. 4 among 158 mutants, there were 13 mutants that showed improved activity. Then colonies showing the improved activity of CYP119 mutants were grown on a bigger scale to confirm their improved activities and for further characterization. The peroxidation activity of these mutants was confirmed by larger scale expression tests (described in the Materials and method section). An increase in peroxidase activity was confirmed for six colonies (Figure S4) in larger scale and these mutants were sent for sequence analysis. Among these mutants, we decided to further characterize the novel T213R/T214I variant of CYP119 that has not been characterized before.

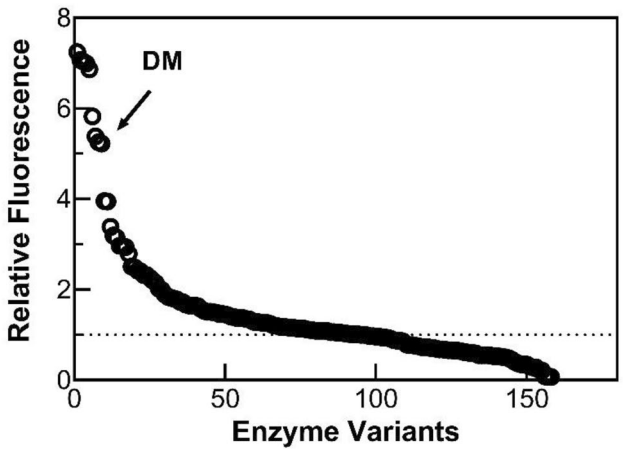

Fig. 4 Relative activities of WT and variants of CYP119, and pET20b samples obtained through Solulyse treatment in 96-well plates plotted in descending order. Relative fluorescence activity obtained from reactions occurred in a single well for each sample. WT CYP119 is set as baseline at 1 (dash line) and T213R/T214I (DM) is indicated with an arrow

Spectral characterization of the T213R/T214I mutant

The optical spectra of WT and T213R/T214I mutant CYP119 as isolated are shown in Fig. 5. WT CYP119 shows maximum Soret absorbance at 414 nm and split alpha–beta (α/β) bands at 531 and 564 nm, similar to previously reported spectra [27]. The T213R/T214I mutation did not result in a significant Soret shift with a Soret maximum at 415 nm; however, there was a broadening of the Soret absorbance and α/β bands (Fig. 5).

Peroxidase activity of WT CYP119 and T213R/T214I mutant with Amplex® Red

The peroxidase activity of purified WT and T213R/T214I mutant of CYP119 was investigated by following the oxidation of Amplex® Red by H_2O_2 with UV–Visible spectroscopy [15]. The changes in the UV–Visible spectra during the reaction of 10 μM Amplex® Red, 1.5 mM H_2O_2, and 1.5 μM WT or T213R/T214I mutant CYP119 at 25 °C are shown in Fig. 6. An increase at 570 nm can be observed during the reaction, this can be attributed to resorufin formation. At the end of the reaction, 7% of Amplex® Red was oxidized by WT in comparison to 60% of Amplex® Red by the T213R/T214I mutant, based on the final concentration of resorufin using the extinction coefficient at 570 nm [16]. Therefore, there was an eightfold increase in the yield of Amplex® Red oxidation by the T213R/T214I mutation.

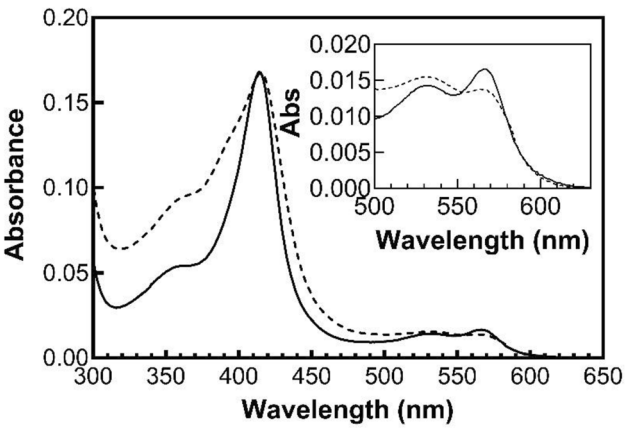

Fig. 5 The comparison of UV–visible spectra of T213R/T214I mutant and WT CYP119 (solid: WT CYP119; dash: T213R/T214I CYP119). Inset: The changes observed in the alpha–beta region

Kinetic analysis of Amplex® Red oxidation by WT CYP119 and T213R/T214I mutant

The kinetic parameters for Amplex® Red oxidation catalyzed by these proteins were investigated (Fig. 7). When Amplex® Red oxidation was monitored in the presence of increasing concentrations of H_2O_2, the k_{cat} obtained was

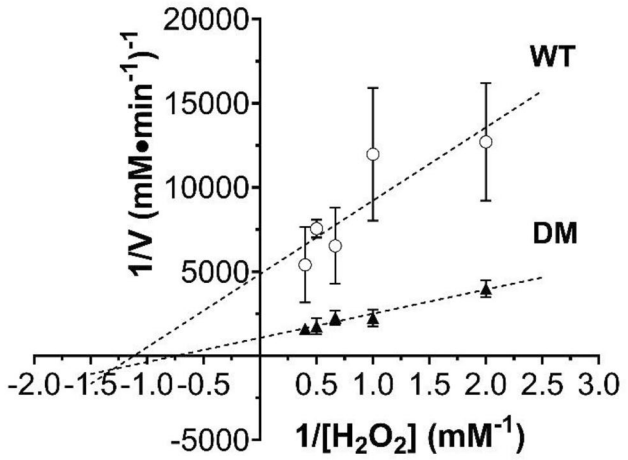

Fig. 7 Determination of the kinetic parameters of Amplex® Red oxidation by H_2O_2 in the presence of WT CYP119 (empty circle) and T213R/T214I variant (DM, filled triangle). Reactions contained 10 μM Amplex® Red, 1.5 μM T213R/T214I or WT CYP119, and 0.5–2.5 mM of H_2O_2 in 50 mM potassium phosphate buffer, pH 7.4

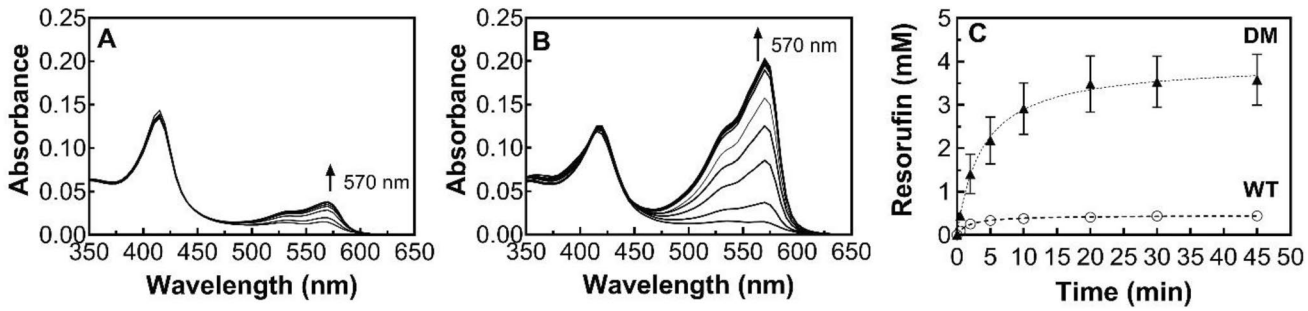

Fig. 6 Changes in the UV–visible spectra during Amplex® Red oxidation by H_2O_2 in the presence of WT (**a**) and T213R/T214I mutant (**b**); the UV–visible spectra taken at 0, 2, 5, 10, 20, 30, and 45 min after addition of H_2O_2. The reaction components were 10 μM Amplex® Red, 1.5 mM H_2O_2, and 1.5 μM enzyme, 1 mM EDTA in 50 mM potassium phosphate buffer at pH 7.4. Time course of changes in resorufin formation at 570 nm for WT CYP119 (empty circle) and T213R/T214I variant (DM, filled triangle) (**c**) in the same reaction

$2.1 \pm 0.3 \times 10^{-3}$ s^{-1} for WT and $1.1 \pm 0.13 \times 10^{-2}$ s^{-1} for the T213R/T214I mutant. There was a fivefold increase in the k_{cat} observed in the T213R/T214I mutant. On the other hand, the K_m observed for H_2O_2 was 0.82 ± 0.46 mM for WT compared to 1.32 ± 0.3 mM for T213R/T214I mutant; showing that the K_m for H_2O_2 was not significantly altered by the mutation.

Styrene epoxidation by WT CYP119 and T213R/T214I mutant

We also investigated the changes in the styrene epoxidation activity of WT and the T213R/T214I mutant of CYP119. The styrene epoxidation was carried out at 25 °C and pH 7.4 in the presence of TBHP as an oxidant. The rate of styrene epoxidation was determined by HPLC analysis with the aid of calibration curves of pure styrene and styrene epoxide. Kinetic constants were obtained by nonlinear fitting analysis with variable concentrations of the substrate styrene (Fig. 8). The k_{cat} obtained were $5 \pm 0.1 \times 10^{-2}$ s^{-1} and $11.7 \pm 0.5 \times 10^{-2}$ s^{-1} for WT and T213R/T214I mutant, respectively. While the K_m obtained for styrene were 14.8 ± 3.2 mM and 14.0 ± 8.3 mM for WT and T213R/T214I, respectively. Therefore, T213R/T214I mutant showed increased k_{cat} of styrene epoxidation without altering the K_m.

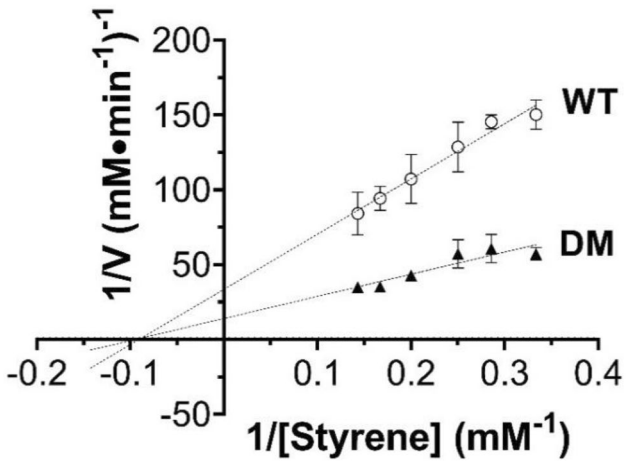

Fig. 8 Determination of the kinetic parameters of styrene epoxidation by variable concentrations of styrene (3–7 mM) in the presence of WT CYP119 (empty circle) and T213R/T214I (DM, filled triangle). Reactions contained variable concentration styrene (3–7 mM), 7 mM TBHP, and 12.5 μM enzyme in 50 mM potassium phosphate buffer at pH 7.4 and 25 °C for 10 min

Reactions of WT CYP119 and T213R/T214I mutant with hydrogen peroxide

To study the reaction of H_2O_2 with WT and T213R/T214I CYP119, we monitored the changes in heme Soret during the reaction of the P450s with H_2O_2. The reaction of 1.5 μM WT with 1.5 mM H_2O_2 resulted in a decrease in the Soret absorbance at 414 nm (Fig. 9a). A 15% decrease in absorbance at 414 nm was observed after incubation of WT with H_2O_2 for 45 min at 25 °C. The observed rate constant for the decrease in Soret absorbance was $1.8 \pm 0.6 \times 10^{-3}$ s^{-1}.

The reaction of T213R/T214I with H_2O_2 was also followed by UV–Vis spectroscopy. The reaction of 1.5 μM T213R/T214I with 1.5 mM H_2O_2 did not result in a significant decrease in maximum Soret absorbance but instead, a narrowing of Soret band was observed (Fig. 9b). The difference spectra show a decrease in 390 nm (Fig. 9b inset). As seen in Fig. 9c the heme Soret maximum 414 nm did not change significantly during the reaction for T213R/T214I, while, for the WT, a significant decrease was observed.

Substrate binding by WT CYP119 and T213R/T214I mutant

Residues Thr213 and Thr214 are located at the active site of the enzyme; therefore, the effects of mutation on the substrate binding to CYP119 were also investigated. Lauric acid was investigated as substrate and the K_d values were

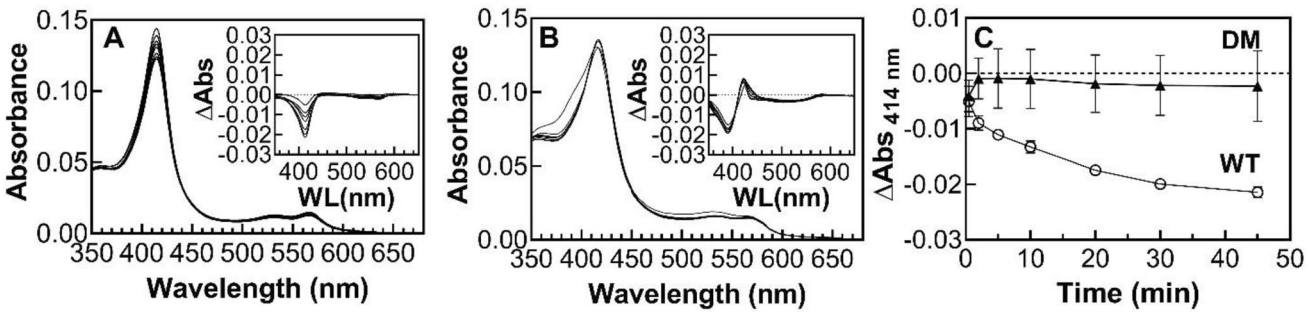

Fig. 9 Changes in the UV–visible spectra during H_2O_2 reaction with WT (**a**) and T213R/T214I mutant (DM) (**b**). Observed spectra at 0, 2, 5, 10, 20, 30, and 45 min. Insets show difference spectra. Reaction contained 1.5 mM H_2O_2, and 1.5 μM enzyme, 1 mM EDTA in 50 mM potassium phosphate buffer at pH 7.4. (**c**) Decrease in 414 nm of WT (empty circle) and DM (filled triangle)

determined from the magnitude of the spin state change which is linked to the magnitude of the absorbance shift (Fig. 10). A larger Soret shift was observed for T213R/T214I mutant compared to WT. In addition, T213R/T214I mutant showed fourfold lower affinity for lauric acid ($K_d = 59.1 \pm 30.2$ μM) compared to WT ($K_d = 16.8 \pm 4.5$ μM).

Molecular modeling and docking of Amplex® Red to WT CYP119 and T213R/T214I mutant

Ligand docking of Amplex® Red molecule into the WT CYP119 (PDB ID: 1F4T) and the T213R/T214I mutant was performed by using the PyRosetta program [24]. The distance between the heme iron atom and the targeted nitrogen atom of Amplex® Red was measured as 6.57 Å for WT CYP119 and 6.26 Å for T213R/T214I mutant (Fig. 11) which indicates that Amplex® Red was located closer to the heme group in T213R/T214I mutant. As shown in Fig. 11, Amplex® Red also forms a hydrogen bond with the backbone of Val258 of T213R/T214I mutant. 1000 rounds of ligand docking were performed for both WT CYP119 and the T213R/T214I mutant. Score distribution histograms are shown in Figure S5. Since the PyRosetta scoring function is a combination of physics-based and knowledge-based information about the structure, the calculated energy scores have the generic unit of REU. Models that have more negative REU scores are generally accepted to be more native-like [28], and thus, docked models with the lowest REU scores were selected to analyze ligand–protein interactions. Lowest REU scores for Amplex® Red docked with WT CYP119 and T213R/T214I mutant models are -517 REU and -1186 REU, respectively.

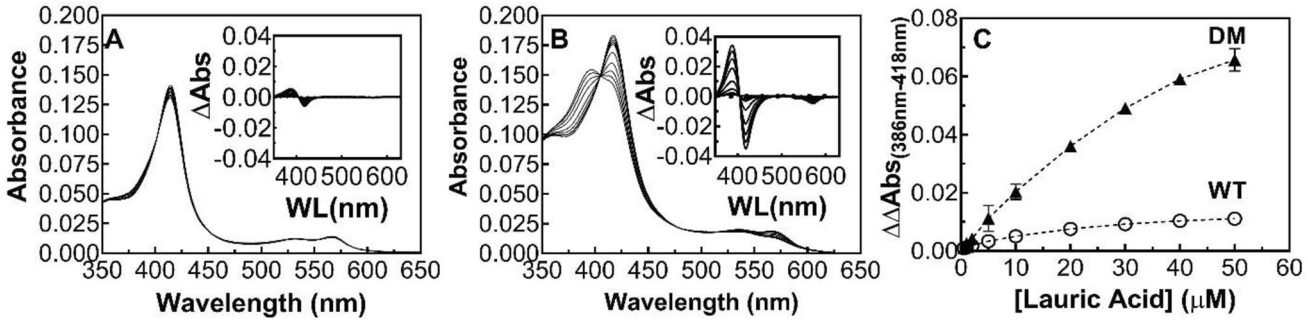

Fig. 10 UV–Visible and difference spectra of WT (**a**) and T213R/T214I mutant (**b**) titrated with saturated lauric acid. Overlay of UV–Visible spectra of 1.5 μM WT CYP119 or T213R/T214I mutant with different concentrations of lauric acid (0.5–50 μM). The insets show difference spectra with increasing lauric acid concentrations. **c** The absorbance shifts observed in 386 nm and 418 nm for lauric acid binding titration of WT CYP119 (empty circle) and T213R/T214I mutant (DM, filled triangle). The absorbance difference between 386 nm and 418 nm [ΔΔAbs (386–418 nm)] versus concentrations of lauric acid plotted by nonlinear fitting

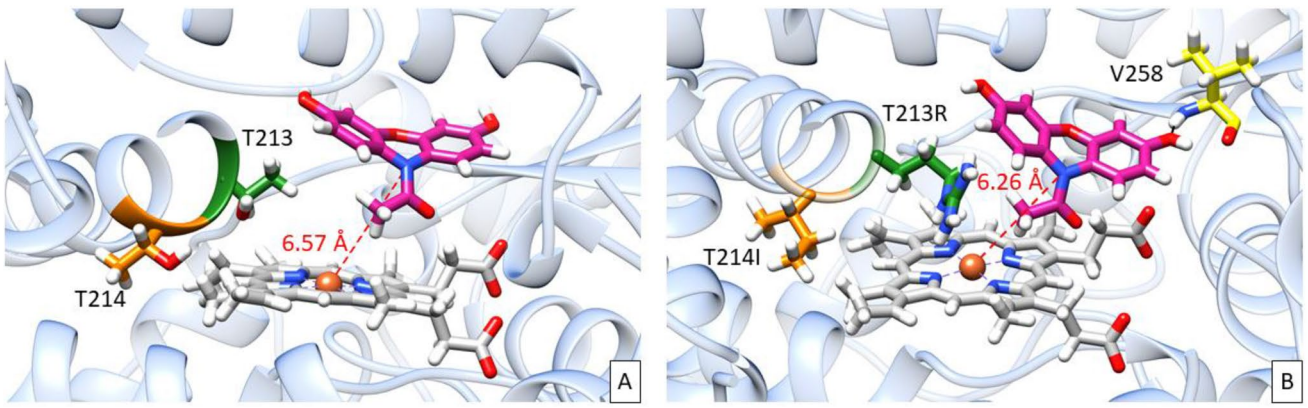

Fig. 11 Docking results of Amplex® Red (pink) with WT CYP119 (PDB ID: 1F4T) and T213R/T214I mutant. **a** WT CYP119 with Amplex® Red. Thr213 (green) and Thr214 (orange) residues are labeled. **b** T213R/T214I mutant with Amplex® Red. Mutant residues are labeled as T213R (green) and T214I (orange). Hydrogen bond between Amplex® Red and Val258 shown is shown as a black line

Discussion

The development of novel P450 enzymes that can utilize H_2O_2 efficiently will open the way for the far wider application of P450s as biocatalysts in industry. Here, we developed an assay that utilizes Amplex® Red peroxidation, to rapidly screen H_2O_2-dependent activity of P450 mutants in cell lysate. This assay was applied to screen a CYP119 mutant library to increase its activity with H_2O_2. Combinatorial Active-site Saturation Test (CAST) method was used to generate the CYP119 mutant library [16]. CYP119 variants with higher activity using H_2O_2 as an oxidant were selected by the rapid screen for Amplex® Red peroxidation. A novel high activity CYP119 variant (T213R/T214I) obtained from the screen was characterized chemically and spectroscopically to gain insights into the mechanism of H_2O_2 reactions with P450 enzymes.

In most activity screens, only a small fraction of all the possible mutated proteins can be screened. Therefore, the CAST method was used to generate a targeted mutant library. Previous studies have shown that Thr213 and Thr214 residues in the active site have key roles for enzyme activity, but they are not critical for thermal stability [11]. Therefore, these residues were selected for targeted mutation.

To improve the catalytic activity of CYP119 with H_2O_2, we developed an activity assay with a substrate whose product can be detected rapidly using fluorescence. Amplex® Red has been used as a highly sensitive and chemically stable fluorogenic probe for enzymatic detection for H_2O_2 [29]. Previous studies have shown that CYP119 can catalyze Amplex® Red peroxidation [15, 18]. The fluorescent product of Amplex® Red peroxidation, resorufin, has a high extinction coefficient and good chemical and photostability; therefore, it is an ideal candidate for rapid screening.

Amplex® Red has commonly been used in assays for the detection of H_2O_2 in conjunction with HRP [29]. Rabe et al. also developed an assay using Amplex® Red with catalase as a reporter enzyme to screen enzyme/peroxide/substrate combinations and assess P450 reactivity with various substrates [17]. The assay developed by Rabe et al. determined activity by monitoring peroxide depletion during the reaction, which makes it prone to interference by other enzymes in the cell lysate; consequently, it can only be used with isolated enzymes. Another Amplex® Red-peroxidase assay was developed for screening the effects of additives and cosolvents on P450 enzymes [30], this assay was also performed with isolated enzymes at micromolar concentrations. The Amplex® Red assays in the literature were not compatible for rapid screening of CYP119 mutants, because they require enzyme isolation due to the complex mechanism of Amplex® Red peroxidation and the low activity of CYP119 with Amplex® Red (k_{cat} for WT CYP119 is 2×10^{-3} s^{-1}, Fig. 7) [31]. Indeed, our initial attempts at monitoring Amplex® Red peroxidation with whole-cell catalysis in cells expressing WT CYP119 did not result in any significant product formation (results not shown). The addition of SoluLyse reagent allowed rapid lysis of cells and substrate conversion by CYP119. In addition, steps in the assay (steps 2 and 3, Fig. 1) had to be optimized to maximize WT or mutant CYP119 concentration in the assay to ensure a significant increase in fluorescence compared to the control. The final CYP119 concentration in the assay was determined to be around 0.5 μM by the Soret absorbance at 415 nm (results not shown). The assay was also optimized by lowering the background fluorescence observed in the negative control, cells containing empty pet20b plasmid, via the addition of 1 mM EDTA (Figure S7). These optimizations allowed rapid screening of mutant colonies for peroxidase activity; to our knowledge, this is the first application of Amplex® Red to detect peroxidase activity of mutants in cell lysate.

We have shown that the conversion of Amplex® Red to resorufin by CYP119 can also be detected in enriched cell lysate without further purification of the protein (Fig. 2). In addition, enrichment of CYP119 was not essential for monitoring activity, simple cell lysis by SoluLyse method was enough for detection of activity (Figure S3). This new method significantly increased the throughput of the assay and 158 mutants of CYP119 were screened for improved peroxidation activity (Fig. 4). This screening led to the identification of six colonies with increased CYP119 peroxidation activity (Figure S4). The six colonies contained five mutations: T213R/T214I, T213R/T214Y, T213D/T214I, T213D/T214N, and T213C/T214C (T213R/T214Y mutation was observed in two different colonies). Among these improved variants, T213R/T214I was selected for further characterization.

Previous studies have indicated that the distal water ligand is more tightly bound in CYP119 compared to other P450s; which makes CYP119 low spin and conversion to high spin is much more difficult [11]. Replacement of Thr214 and Thr213 with large amino acids considerably increased the proportion of high spin. The improved variant, T213R/T214I, showed broadening of the Soret peak, which can be explained by changes in the spin state of the heme iron (Fig. 5).

When substrate binding of T213R/T214I mutant is compared to WT, in addition to changes in affinity for lauric acid, binding of substrate to T213R/T214I mutant results in a more significant increase in 390 nm absorbance compared to WT (Fig. 9). This shift in Soret absorbance can also be attributed to changes in the spin state of the heme iron to high spin. Taken together, the conversion of the

heme iron in T213R/T214I to high spin is easier and the protein is most likely isolated in a mixed spin state rather than low spin. This result is consistent with the previous studies that indicated that the Thr214 residue is involved in controlling the spin state of the heme iron [11]. In addition, alignment of the active site of WT CYP119 with modeled T213R/T214I variant (Figure S6) shows that the T213R mutation displaces the distal water molecule, which will also lead to changes in the resting spin state of the heme iron.

To test if the T213R/T214I variant will show increased Amplex® Red peroxidation activity when isolated and to investigate the changes in Amplex® Red peroxidation mechanism, the reaction of WT and T213R/T214I mutant with Amplex® Red and H_2O_2 was investigated. The mutant showed an eightfold increase in Amplex® Red peroxidation yield compared to WT. When the reaction kinetics were followed with increasing concentrations of H_2O_2, a fivefold increase in k_{cat} was observed for the T213R/T214I mutant (Fig. 7). On the other hand, the K_m for H_2O_2 was not affected by the mutation.

The screen was designed to select for increased Amplex® Red peroxidation by H_2O_2. The reasoning behind the screen was to utilize the excellent probe properties of resorufin to identify general increased reactivity towards oxidations by H_2O_2. Increased Amplex® Red peroxidation activity can stem from two changes in the active site: increased activity towards H_2O_2 and increased affinity for Amplex® Red. Since kinetic analysis of the peroxidation reaction was not performed under saturating concentrations of Amplex® Red, the changes in k_{cat} can be due to changes in affinity for Amplex® Red. Docking studies were performed to test for changes in affinity for Amplex® Red. Indeed, docking results showed lower binding energy (− 1186 REU for T213R/T214I vs -517 REU for WT), therefore, increased affinity for Amplex® Red for the improved variant. In addition, the distance between the heme iron and targeted nitrogen atom of Amplex® Red decreased for the improved mutant (6.57 Å for WT vs 6.26 Å for T213R/T214I, Fig. 11), which may lead to more efficient electron transfer.

To understand if the mutant CYP119s selected by the assay also show increased activity for other substrates, epoxidation of styrene by the T213R/T214I mutant was investigated. Previous studies have shown that TBHP is a better electron acceptor than H_2O_2 for styrene epoxidation by CYP119; therefore, TBHP was used as an oxidant rather than H_2O_2 in styrene epoxidation [15]. Under these conditions T213R/T214I showed twofold higher catalytic activity for styrene epoxidation ($k_{cat} = 1.2 \times 10^{-1}$ s^{-1} for T213R/T214I vs 5×10^{-2} s^{-1} for WT). While the affinity for styrene was not altered by mutation ($K_m = 14$ mM for T213R/T214I vs 14.8 mM for WT). The styrene epoxidation kinetics of WT CYP119 is within the range of previous observations ($k_{cat} = 1 \times 10^{-2}$ s^{-1} with H_2O_2 as the oxidant at 30 °C [11], $k_{cat} = 1.3$ s^{-1} with TBHP as the oxidant at 70 °C [15]).

In previous studies, styrene epoxidation of CYP119 has also been significantly improved by single mutation of T213E [32]. Indeed, the k_{cat} for styrene epoxidation by T213E CYP119 was shown to be 0.27 s^{-1} at 70 °C in the presence of 60 mM H_2O_2. The observed k_{cat} for T213E appears to be twofold higher than for T213R/T214I; however, the reactions were performed under different conditions (25 °C vs 70 °C and oxidant 7 mM TBHP vs 60 mM H_2O_2). Consequently, it is not possible to compare these mutants directly. Evidence from previous studies have shown that changing oxidant and increasing temperature can lead to a tenfold increase in k_{cat} for CYP119 [11, 14].

In this study, the CYP119 mutant library was generated using the NDT codon degeneracy which utilizes 12 amino acids (Phe, Leu, Ile, Val, Tyr, His, Asn, Asp, Cys, Arg, Ser, and Gly). Therefore, the mutant library does not contain the T213E mutation, but the T213D mutation was tested. Indeed, two of the five mutants that show higher activity from the Amplex® Red screen are the T213D/T214I and T213D/T214N mutants (Figure S4). While the activity of T213D CYP119 has not been tested previously, the Ala245 residue is located at the same position in $P450_{SP\alpha}$, and mutational studies by Shoji et al. have shown that A245D $P450_{SP\alpha}$ also has increased styrene epoxidation activity (but not as high as A245E $P450_{SP\alpha}$) [32]. The increased activity in A245E $P450_{SP\alpha}$ was explained by the carboxylate group of A245E in the distal pocket acting as an acid–base catalyst in the generation of the active species during the reaction with H_2O_2 similar to the substrate-bound state of $P450_{SP\alpha}$ [32]. The carboxylate group of the substrate in $P450_{SP\alpha}$ is thought to abstract a peroxide proton leading to the heterolytic cleavage of the peroxide to form the active oxygen species compound I [33]. While A245E $P450_{SP\alpha}$ and T213E CYP119 can accelerate the reaction via a similar mechanism, T213R CYP119 must have a different mechanism.

It is important to note that two of the five mutants that show higher activity contain the T213R mutation, T213R/T214I and T213R/T214Y, (Figure S4), we can thus conclude that the T213R mutation is important for increased activity. One possible explanation for the increase in activity could be that Arg213 is involved in an interaction with a close-by carboxylic acid similar to Arg241 in $P450_{SP\alpha}$ with the carboxylic acid group of the substrate. However, a detailed analysis of the active site did not show any evidence of any such interaction. One conceivable outcome of the T213R mutation is an increase in the polarity of the heme pocket; peroxidases and P450s that employ H_2O_2 as an oxidant such as $P450_{SP\alpha}$ and $P450_{BS\beta}$ possess more polar heme pocket compared to the nonpolar heme pockets observed in other P450s, such as P450BM3 [34]. While Arg213 cannot abstract a proton from the peroxide, its interactions with

water molecules in the distal pocket may lead to acid–base catalysis that promotes heterolysis of the peroxide O–O bond. In peroxidases such as HRP and cytochrome *c* peroxidase, the distal arginine is involved in stabilizing the developing negative charge on the leaving oxygen atom thus promoting heterolysis. The arginine mutants in peroxidases also show different reactivity and stability of compound I [34]. More mechanistic studies are necessary to understand the role of the T213R mutation in the peroxidase activity of CYP119.

The reaction of T213R/T214I with H_2O_2 was also investigated to understand how the mutation affected reactivity towards peroxides in the absence of other substrates. T213R/T214I heme showed increased stability towards degradation by H_2O_2 since no significant decrease in Soret absorbance is observed during its reaction with H_2O_2 (Fig. 9). This observation is consistent with the previous studies where Thr213 and Thr214 mutations were heme bleached more slowly by H_2O_2 [11]. Therefore, increased Amplex® Red peroxidation activity was due to both changes in substrate affinity and reactivity towards peroxides.

The role of Thr213 in the activation of ferric peroxide complex during the reaction of CYP119 with H_2O_2 is not yet completely understood. Previous studies indicated that the accessibility of H_2O_2 was more crucial than the spin state of the heme iron [11]. However, our results show that the presence of a bulky charged arginine residue at Thr213 position can also increase peroxidation activity; therefore, accessibility to H_2O_2 may not be as important as previously thought.

Taken together, Amplex® Red peroxidation activity assay can select for enzymes that show higher activity with peroxides. However, because Amplex® Red is used as a substrate inherently the assay will also select for enzymes with altered substrate selectivity. This may be an asset as one of the limitations of microbial P450s is their limited substrate scope, and future studies will focus on changes in substrate selectivity of the improved variant T213R/T214I.

Conclusion

This study entails the development of an assay to detect the peroxidation activity of P450s in cell lysate and screening CYP119 mutants to improve its H_2O_2-dependent activity. CAST method was employed in the generation of a CYP119 mutant library by targeting Thr213 and Thr214 residues for mutation. An effective screening method that utilized Amplex® Red as a substrate was developed to determine variants displaying higher peroxidation activity while employing H_2O_2 as oxidant. This allowed the rapid screening of 158 variants of CYP119 in 96-well plates; five mutants showed higher peroxidase activity compared to WT CYP119. Among the improved variants, the novel T213R/T214I mutant was selected for further characterization. T213R/T214I displayed increased activity for styrene epoxidation in addition to Amplex® Red peroxidation. In addition, the heme iron in T213R/T214I mutant demonstrated higher stability towards H_2O_2-dependent degradation. While T213R/T214I is not the first CYP119 mutant that shows increased peroxidation activity, the activation mechanism of T213R mutation is novel and future studies are necessary to elucidate the molecular mechanism. Taken together, P450 mutants with higher peroxidation activity can be developed by screening with Amplex® Red as a substrate; this method was used to identify a novel variant of CYP119 with significantly higher peroxidation activity. Characterization of the higher activity T213R/T214I variant will contribute to our understanding of P450s H_2O_2-dependent oxidation reactions.

Acknowledgements This work was supported by The Scientific and Technological Research Council of Turkey [TUBİTAK, 116Z380]. We thank Ali Oğuz Büyükkileci for his help with the HPLC analysis and Çağlar Karakaya for allowing access to ultrasonicator instrument.

Compliance with ethical standards

Conflict of interest The authors declare no conflict of interest.

References

1. Denard CA, Ren H, Zhao H (2015) Improving and repurposing biocatalysts via directed evolution. Curr Opin Chem Biol 25:55–64
2. McLean KJ et al (2015) Single-step fermentative production of the cholesterol-lowering drug pravastatin via reprogramming of Penicillium chrysogenum. Proc Natl Acad Sci 112(9):2847–2852
3. Bracco P, Janssen DB, Schallmey A (2013) Selective steroid oxyfunctionalisation by CYP154C5, a bacterial cytochrome P450. Microb Cell Fact 12(1):95
4. Duport C et al (1998) Self-sufficient biosynthesis of pregnenolone and progesterone in engineered yeast. Nat Biotechnol 16(2):186–189
5. Szczebara FM et al (2003) Total biosynthesis of hydrocortisone from a simple carbon source in yeast. Nat Biotechnol 21(2):143–149
6. Hrycay EG, Bandiera SM (2012) The monooxygenase, peroxidase, and peroxygenase properties of cytochrome P450. Arch Biochem Biophys 522(2):71–89
7. Shoji O, Watanabe Y (2014) Peroxygenase reactions catalyzed by cytochromes P450. J Biol Inorg Chem 19(4–5):529–539
8. Lee JW et al (2011) Microbial production of building block chemicals and polymers. Curr Opin Biotechnol 22(6):758–767
9. Joo H, Lin Z, Arnold FH (1999) Laboratory evolution of peroxide-mediated cytochrome P450 hydroxylation. Nature 399(6737):670–673
10. Matsuura K et al (2004) Structural and functional characterization of "laboratory evolved" cytochrome P450cam mutants showing enhanced naphthalene oxygenation activity. Biochem Biophys Res Commun 323(4):1209–1215
11. Koo LS et al (2000) The active site of the thermophilic CYP119 from Sulfolobus solfataricus. J Biol Chem 275(19):14112–14123

12. Brock TD et al (1972) Sulfolobus: a new genus of sulfur-oxidizing bacteria living at low pH and high temperature. Archiv für Mikrobiologie 84(1):54–68
13. Yano JK et al (2000) Crystal structure of a thermophilic cytochrome P450 from the archaeon Sulfolobus solfataricus. J Biol Chem 275(40):31086–31092
14. Lim YR et al (2010) Regioselective oxidation of lauric acid by CYP119, an orphan cytochrome P450 from Sulfolobus acidocaldarius. J Microbiol Biotechnol 20(3):574–578
15. Rabe KS, Kiko K, Niemeyer CM (2008) Characterization of the peroxidase activity of CYP119, a thermostable P450 from *Sulfolobus acidocaldarius*. ChemBioChem 9(3):420–425
16. Reetz MT et al (2005) Expanding the range of substrate acceptance of enzymes: combinatorial active-site saturation test. Angew Chem Int Ed 44(27):4192–4196
17. Rabe KS et al (2009) Screening for cytochrome p450 reactivity by harnessing catalase as reporter enzyme. ChemBioChem 10(4):751–757
18. Aslantas Y, Surmeli NB (2019) Effects of N-terminal and C-terminal polyhistidine tag on the stability and function of the thermophilic P450 CYP119. Bioinorg Chem Appl 2019:8080697
19. Ivanec-Goranina R, Kulys J (2008) Kinetic study of peroxidase-catalyzed oxidation of 1-hydroxypyrene. Development of a nanomolar hydrogen peroxide detection system. Central Eur J Biol 3(3):224
20. Mishin V et al (2010) Application of the Amplex red/horseradish peroxidase assay to measure hydrogen peroxide generation by recombinant microsomal enzymes. Free Radic Biol Med 48(11):1485–1491
21. Zhao B, Summers FA, Mason RP (2012) Photooxidation of Amplex Red to resorufin: implications of exposing the Amplex Red assay to light. Free Radic Biol Med 53(5):1080–1087
22. Suzuki R, Hirakawa H, Nagamune T (2014) Electron donation to an archaeal cytochrome P450 is enhanced by PCNA-mediated selective complex formation with foreign redox proteins. Biotechnol J 9(12):1573–1581
23. Koo LS et al (2002) Enhanced electron transfer and lauric acid hydroxylation by site-directed mutagenesis of CYP119. J Am Chem Soc 124(20):5684–5691
24. Chaudhury S, Lyskov S, Gray JJ (2010) PyRosetta: a script-based interface for implementing molecular modeling algorithms using Rosetta. Bioinformatics 26(5):689–691
25. Pettersen EF et al (2004) UCSF Chimera—a visualization system for exploratory research and analysis. J Comput Chem 25(13):1605–1612
26. Schneider TD, Stephens RM (1990) Sequence logos: a new way to display consensus sequences. Nucleic Acids Res 18(20):6097–6100
27. McLean MA et al (1998) Characterization of a cytochrome P450 from the acidothermophilic Archaea *Sulfolobus solfataricus*. Biochem Biophys Res Commun 252(1):166–172
28. Misura KM et al (2006) Physically realistic homology models built with ROSETTA can be more accurate than their templates. Proc Natl Acad Sci 103(14):5361–5366
29. Zhou M et al (1997) A stable nonfluorescent derivative of resorufin for the fluorometric determination of trace hydrogen peroxide: applications in detecting the activity of phagocyte NADPH oxidase and other oxidases. Anal Biochem 253(2):162–168
30. Rabe KS et al (2010) Peroxidase activity of bacterial cytochrome P450 enzymes: modulation by fatty acids and organic solvents. Biotechnol J 5(8):891–899
31. Towne V et al (2004) Complexities in horseradish peroxidase-catalyzed oxidation of dihydroxyphenoxazine derivatives: appropriate ranges for pH values and hydrogen peroxide concentrations in quantitative analysis. Anal Biochem 334(2):290–296
32. Shoji O et al (2016) A substrate-binding-state mimic of H_2O_2-dependent cytochrome P450 produced by one-point mutagenesis and peroxygenation of non-native substrates. Catal Sci Technol 6:5806–5811
33. Lee DS et al (2003) Substrate recognition and molecular mechanism of fatty acid hydroxylation by cytochrome P450 from *Bacillus subtilis*. Crystallographic, spectroscopic, and mutational studies. J Biol Chem 278(11):9761–9767
34. Poulos TL (2014) Heme enzyme structure and function. Chem Rev 114(7):3919–3962